Conceptual Design of Monocolumn Production and Storage With Dry Tree Capability

Article *in* Journal of Offshore Mechanics and Arctic Engineering · September 2010

DOI: 10.1115/1.4001429

CITATIONS
5

READS
198

5 authors, including:

Rodolfo Trentin Gonçalves
The University of Tokyo
73 PUBLICATIONS **304** CITATIONS
SEE PROFILE

Edgard Malta
University of São Paulo
16 PUBLICATIONS **33** CITATIONS
SEE PROFILE

Kazuo Nishimoto
University of São Paulo
110 PUBLICATIONS **332** CITATIONS
SEE PROFILE

Rodolfo T. Gonçalves
e-mail: rodolfo_tg@tpn.usp.br

Fabio T. Matsumoto
e-mail: fabio_matsumoto@tpn.usp.br

Edgard B. Malta
e-mail: edgard@tpn.usp.br

Higor F. Medeiros
e-mail: higorfm@gmail.com

Kazuo Nishimoto
e-mail: knishimo@usp.br

TPN-Numerical Offshore Tank,
Department of Naval Architecture and Ocean Engineering,
University of São Paulo,
Avenue Prof. Mello Moraes, 2231,
Cidade Universitária,
São Paulo, SP, 05508-900, Brazil

Conceptual Design of Monocolumn Production and Storage With Dry Tree Capability[1]

A new concept and a preliminary study for a monocolumn floating unit are introduced, aimed at exploring and producing oil in ultradeep waters. This platform, which combines two relevant features—great oil storage capacity and dry tree production capability—comprises two bodies with relatively independent heave motions between them. A parametric model is used to define the main design characteristics of the floating units. A set of design alternatives is generated using this procedure. These solutions are evaluated in terms of stability requirements and dynamic response. A mathematical model is developed to estimate the first order heave and pitch motions of the platform. Experimental tests are carried out in order to calibrate this model. The response of each body alone is estimated numerically using the WAMIT® code. This paper also includes a preliminary study on the platform mooring system and appendages. The study of the heave plates presents the gain, in terms of decreasing the motions, achieved by the introduction of the appropriate appendages to the platform. [DOI: 10.1115/1.4001429]

Keywords: floating unit design, monocolumn platform, hydrodynamic behavior, hydrodynamic appendages, model tests

1 Introduction

In recent years, Brazil has been setting water depth records in offshore oil exploration, with new reserves of oil and gas having been discovered and confirmed by PETROBRAS, Petróleo Brasileiro, RJ, Brazil. This scenario makes the oil industry develop and modernize itself in order to meet the huge market demand. A continuous challenge for the industry is to reduce production costs in ultradeep water areas.

In this context, a new concept of a floating unit for exploration and production of oil in ultradeep waters is proposed. This concept provides great storage capacity and dry tree production capability. Both characteristics aim to reduce the costs of oil production. In order to obtain dry completion, reduced motions of the intervention system are required. A similar concept to meet these requirements was proposed by Poldervaart and Pollack [1], and Reyes et al. [2].

This concept comprises two bodies, with relatively independent heave motions between them, where one body (monocolumn with moonpool) works as a storage unit and the other one as a dry completion unit located inside the moonpool. The coupled heave motion between them is due only to the hydrodynamical nature; details are presented as follows. The concept feasibility, with high storage capability and reduced motion, is also discussed. Details about the monocolumn concept are presented in Refs. [3,4].

Section 2 presents the design premises as well as the main characteristics of the new concept. It is followed by Sec. 3, which describes the model tests and the numeric models used to describe the platform response, as well as the calibration of the numeric model based on the experimental results. Subsequently, Sec. 4 discusses the philosophy used to design the platform. Section 5 presents the conclusions regarding the feasibility of the new concept.

2 Design Conception

In this section, the design premises and the main features of the new concept are outlined.

2.1 New Concept. The new concept, as illustrated in Fig. 1, is characterized by the presence of two bodies.

The main body is similar to a monocolumn platform with a moonpool, which has the following functions: (i) production storage, (ii) supports the process plant, intervention tower, and living quarters, and (iii) contains the connection points to the mooring lines.

The inner body, which is inside the main body moonpool, has the following functions: (i) supports the dry tree and (ii) connects the risers system. The risers are top tension riser (TTR) configurations. Pretension of the risers are provided by the inner body buoyancy.

The two bodies need to have relatively independent vertical motions. This motion decoupling is provided by a rolling system, which allows a free vertical motion of the inner body inside the main body moonpool.

2.2 Design Basis. The design basis for the new concept is as follows:

- Campos basin (Brazil) environment
- ultradeep water
- storage capacity
- eight radial tanks
- nine risers (11.75 in. (298.45 mm) outer diameter (OD) and 1.25 in. (31.75 mm) wall thickness)
- spacing between the moonpool walls and the inner body external side is 3 m, which is assumed wide enough to accommodate the rolling system
- moonpool diameter large enough to support the deck area for the dry tree
- taut-leg mooring lines are required due to the limited offset allowed (5% of water depth)

[1]This paper includes OMAE2008-57440: "Conceptual Design of Floating Production and Storage with Dry Tree Capability" and OMAE2008-57410: "The Influence at Vertical First Order Motions Using Appendages in a Monocolumn Platform" presented in the 27th International Conference on Offshore Mechanics and Arctic Engineering, 2008, Estoril, Portugal.

Contributed by the Ocean Offshore and Arctic Engineering Division of ASME for publication in the JOURNAL OF OFFSHORE MECHANICS AND ARCTIC ENGINEERING. Manuscript received February 6, 2009; final manuscript received October 23, 2009; published online September 23, 2010. Assoc. Editor: Celso P. Pesce.

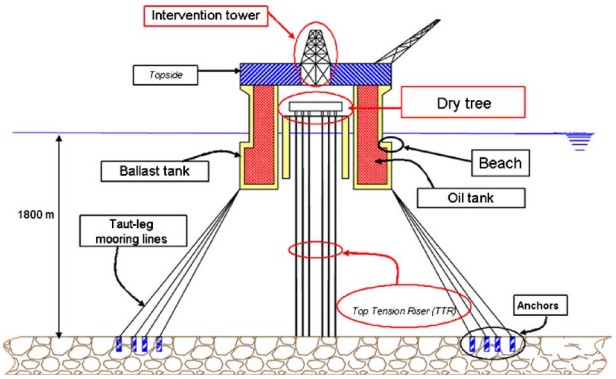

Fig. 1 Schematic of the new concept

- 70% or more of the operation time in fixed ballast condition

2.3 Environment Conditions. The environment conditions are typical of the Campos basin in Brazil, and a water depth equal to 1,800 m is assumed. Three wave spectra have been assumed to correspond to 1 year, 10 year, and 100 year sea levels.

- sea 1: Joint North Sea Wave Project (JONSWAP) spectrum $\gamma=1.76$, $H_s=6.37$ m, $T_p=13.93$ s
- sea 2: JONSWAP spectrum $\gamma=1.71$, $H_s=7.16$ m, $T_p=14.78$ s
- sea 3: JONSWAP spectrum $\gamma=1.66$, $H_s=7.84$ m, $T_p=15.55$ s

2.4 Risers System. The steel risers are TTR. A heave motion compensation system is assumed not to be required.

TTR risers should not be compressed; therefore, they must be pretensioned. Pretension of risers is provided by the buoyancy of the inner body. If required, tension on risers could be modified, either by applying tensioners on the risers extremities or by performing a ballast operation of the inner body.

Pretension was calculated for 1.6 m vertical displacement. The result is a pretension equal to a 256.8 ton/riser.

2.5 Hull Dimensions. The main body is similar to a monocolumn with a moonpool and is designed in such a way that its beach (change in the external hull diameter; see Fig. 1) is always below the water line for the different loading conditions. The moonpool has parallel walls to accommodate the inner body within it. The main body is double sided and follows the rules of Marine Pollution (MARPOL) 73/78 [5].

The inner body is cylindrical and has ballast tanks. The buoyancy of the inner body should support the dry tree weight and the risers' pretension.

2.6 Mooring System. The mooring lines present a taut-leg configuration due to limited offset. The line consists of three segments: (i) 50 m segment on the bottom chain; (ii) 50 m on the top spiral strand segment; and (iii) polyester segment with a post-evaluated length. The polyester segment is calculated according to the layout of the mooring system (number and angles of the lines).

3 Model Tests and Numerical Calibration

3.1 Model Tests—General Description. The test matrix was accomplished at the Department of Naval Architecture and Ocean Engineering basin, at the University of São Paulo in July 2007. The model scale was 1:150. The models are shown in Fig. 2. The prototype dimensions for the main and inner bodies are presented in Figs. 3 and 4, respectively.

The experiments were carried out in regular and transient waves; there were also decay tests in the heave and pitch motions. The tests were performed with and without the inner body inside the main body moonpool, in order to investigate the influence of the main body on the inner body response.

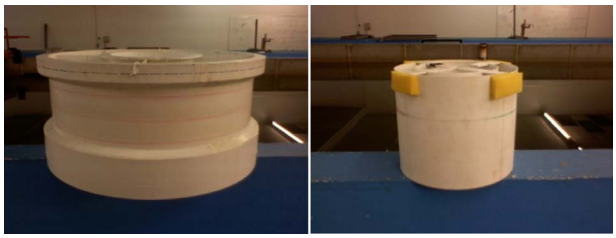

Fig. 2 Models to scale

All the tests in waves were carried out without the presence of mooring lines or risers. Three different platform configurations were considered in the tests, as follows:

- SS1: the main body alone
- CI1: the inner body alone
- SS2: the main body and inner body together

Figure 5 shows the settings for configuration SS2.

3.2 Model Tests—Results Highlights. *Natural periods.* The natural periods, which are derived from the decay tests, are shown in Tables 1 and 2, for the heave and pitch motions, respectively. The decay tests were performed without risers or mooring lines.

The results show that the main body natural periods do not change in the presence of the inner body. The heave natural period of the inner body changes in the presence of the main body, due to the fluid flow between them.

First order motions. The first order motions were evaluated through the response amplitude operator (RAO) obtained from the model test submitted to waves.

The experimental results are presented along with the numerical RAO for comparison purposes in Figs. 7–10.

3.3 Numerical Model—General. The numerical model used in this paper was suggested by Malta et al. [6] and Torres et al. [7,8], and was developed using the WAMIT® code (see Ref. [9]). The WAMIT® code applies a potential theory to evaluate the motions of each body separately. Figure 6 shows a mesh example of the model.

So to evaluate the inner body dynamics in the presence of the main body, the following formulation was used:

$$\mathrm{RAO}^{*}_{\mathrm{inner}}(\omega) = \mathrm{RAO}_{\mathrm{moonpool}}(\omega) \cdot \mathrm{RAO}_{\mathrm{inner}}(\omega) \tag{1}$$

where $\mathrm{RAO}^{*}_{\mathrm{inner}}$ is the inner body RAO in the presence of the main body, $\mathrm{RAO}_{\mathrm{moonpool}}$ is the free surface elevation at the main body moonpool (without the presence of inner body), $\mathrm{RAO}_{\mathrm{inner}}$ is the inner body RAO alone, and ω is the frequency wave.

This formulation assumes that (i) the inner body is excited by the elevation of the main body moonpool and (ii) the free surface of the main body moonpool is not disturbed by the inner body (diffraction/radiation waves are neglected).

The simplification was made to reduce the computational time of the numerical model developed in the WAMIT® code using three different coupled bodies (main body, inner body, and free surface of the internal moonpool). Using the formulation above, the numerical model was developed for each body separately (main body+free surface and inner body+free surface). Also, the close distance between the main and inner bodies causes numerical errors in the potential calculations due to the proximity of the sources in the low-order model. The numerical models are calibrated based on the experimental results.

3.4 Numerical Model—Result Highlights. The numerical and experimental RAOs are presented below. The full lines

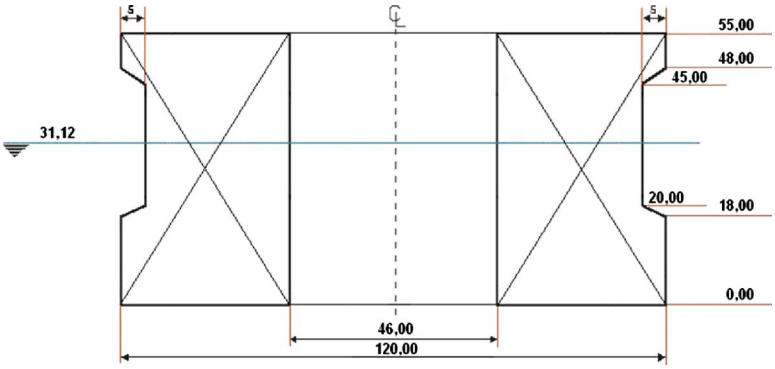

Fig. 3 Prototype dimensions—main body

represent the numerical results and the dashed lines represent the experimental ones.

Figure 7 illustrates the RAO comparison for the main body heave motion without the inner body, while Fig. 8 illustrates the comparison for the heave motion of the inner body alone.

Figure 9 shows the comparison between the numerical and experimental results for the heave motion of the inner body in the presence of the main body. The numerical results in this case were obtained by using Eq. (1).

Figure 10 shows the comparison between the numerical and experimental results for the pitch motion of the main body, with and without the inner body. The results show that the inner body does not influence the pitch motion of the main body. The pitch motion of the inner body in the presence of the main body is considered the same as the pitch motion of the main body due to the proposed mechanical rolling system.

3.5 Numerical Versus Model Tests. It can be seen that there is a fair agreement between the experimental results and the calibrated numerical ones. Therefore, the proposed model (Eq. (1)) will be used to evaluate the inner body dynamics inside the main body.

4 Design Procedure

The methodology adopted to develop the preliminary design of the new system concept is presented in this section, considering its operation in Brazilian offshore oil fields.

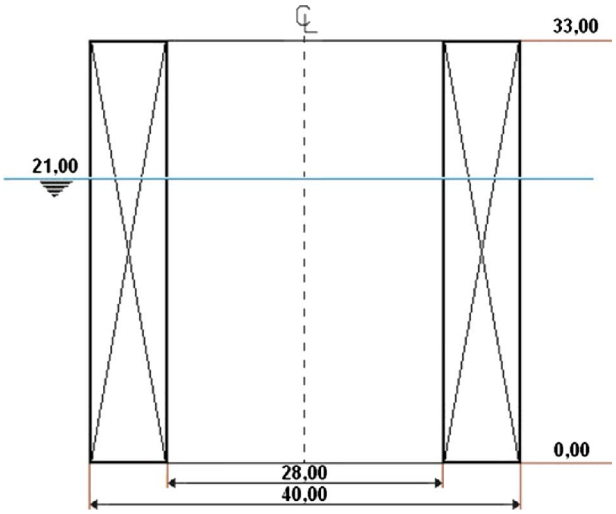

Fig. 4 Prototype dimensions—inner body

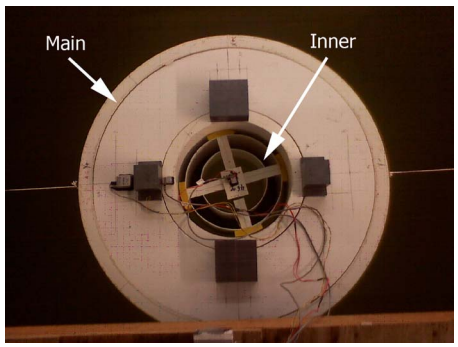

Fig. 5 Experimental setup—SS2

Table 1 Natural periods—heave motion

Setup	Natural period main body (s)	Natural period internal body (s)
SS1	17.56	-
CI1	-	9.75
SS2	17.45	9.19

Table 2 Natural periods—pitch motion

Setup	Natural period main body (s)	Natural period internal body (s)
SS1	22.49	-
CI1	-	11.06
SS2	22.38	-

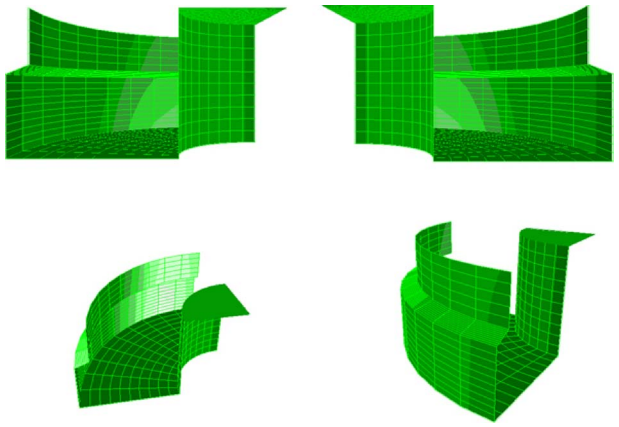

Fig. 6 Mesh of the main body

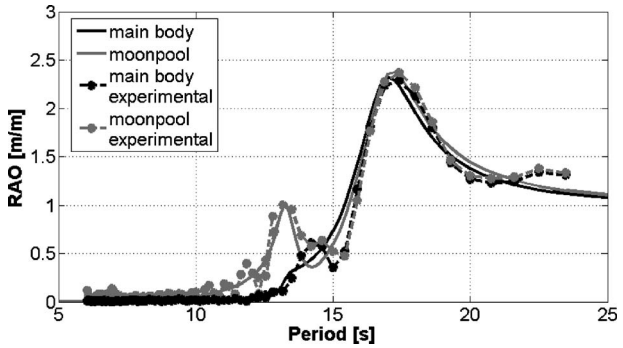

Fig. 7 Comparison of the heave motion RAO—main body

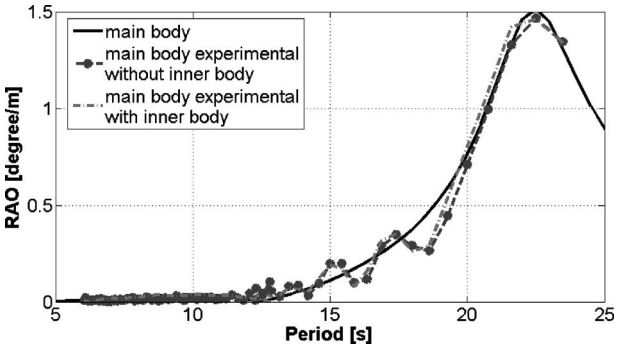

Fig. 10 Comparison of the pitch motion RAO—main body

4.1 General Design Requirements. The general design requirements are as follows: (i) Brazilian environment, (ii) storage capacity of 800,000 bbls, and (iii) topside capacity of 100,000 bopd.

4.2 Design Environmental Conditions. The centenary (100-year return period) sea spectrum is used to develop the system design; nevertheless, the system performance is also investigated in three sea conditions, as was previously mentioned. The parameters of these conditions are defined in Table 3. The wind and current characteristics are shown in Tables 4 and 5, respectively.

4.3 Hull Design. A parametric model, which takes into account the design premises and requirements, was used to generate different hull alternatives.

The parametric model has as its main feature the division of the platform in slices, as illustrated in Fig. 11. The evaluation of the system characteristics is performed for each slice individually and, afterwards, the results are integrated to provide the characteristics of the entire system. The design variables referring to the body dimensions are defined in Fig. 12.

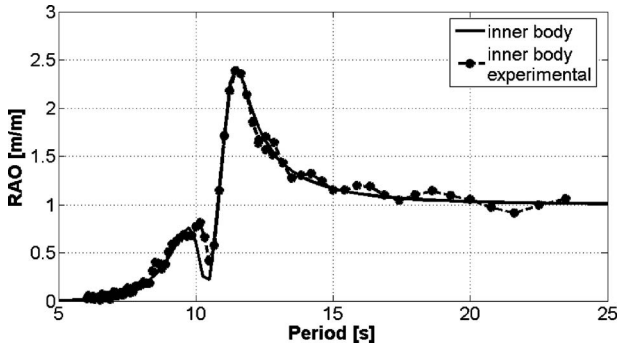

Fig. 8 Comparison of the heave motion RAO—inner body

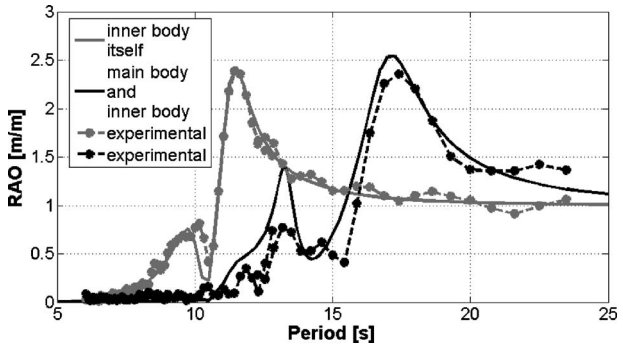

Fig. 9 Comparison of the heave motion RAO—inner body with main body

The dimensions and subdivision of the oil and ballast tanks are in accordance with the MARPOL 73/78 requirements. The design alternatives generated by the parametric design satisfy the minimum stability criteria and others as follows:

- $GM > 1.0$ m

Table 3 Wave conditions in the Campos basin

	1 yr.		10 yrs.		100 yrs.	
Sector	T_p (s)	H_s (m)	T_p (s)	H_s (m)	T_p (s)	H_s (m)
N	8.81	4.44	9.20	4.74	9.58	5.01
NE	9.13	4.55	9.47	4.88	9.77	5.17
E	9.35	3.72	9.90	4.34	10.40	4.87
SE	10.90	4.81	10.28	5.72	11.63	6.53
S	12.65	5.14	13.54	6.19	14.35	7.10
SW	13.93	6.37	14.78	7.16	15.55	7.84
W	7.91	3.21	8.22	3.57	8.51	3.88
NW	7.91	3.21	8.22	3.57	8.51	3.88

Table 4 Wind conditions in the Campos basin

	Wind velocity (m/s)		
Sector	1 yr.	10 yrs.	100 yrs.
N	17.76	23.22	28.54
NE	18.64	23.91	29.11
E	15.18	20.42	25.57
SE	15.76	21.95	28.05
S	17.52	24.43	31.24
SW	17.31	24.50	31.58
W	16.17	24.08	31.88
NW	13.50	19.29	25.00

Table 5 Current conditions in the Campos basin

	Current velocity (m/s)		
Sector	1 yr.	10 yrs.	100 yrs.
N	1.47	1.76	2.06
NE	1.47	1.70	1.89
E	0.81	0.94	1.04
SE	0.97	1.13	1.26
S	1.12	1.34	1.54
SW	0.81	0.93	1.03
W	0.80	0.97	1.13
NW	1.41	1.62	1.79

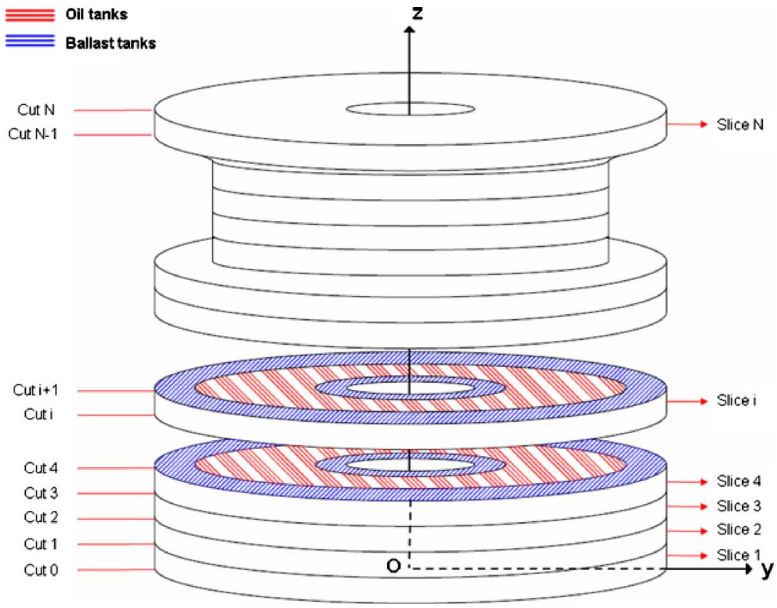

Fig. 11 Discretization of the floating unit in slices

- Rint $>$ 23.0 m, in order to provide dry tree production capability
- $Dp_{max} < 20.0$ m, related to the minimum draft of the main body, in order to avoid hawser disconnection (see Fig. 13)
- $Dp_{min} > 8.0$ m, related to the maximum draft of the main body, in order to avoid shock between the two bodies (see Figs. 13 and 14)
- loading conditions for the maximum and minimum drafts, which meet a system operation period greater than 70% in fixed ballast

The evaluation of the hull mass and inertia takes into account the structural mass (computed from the model presented by Malta et al. [10]), as well as the oil and ballast; the latter two components depend on the loading condition.

The fixed ballast condition with enough volume of oil to meet the Dp_{max} constraint is defined as LC2. The fixed ballast condition with enough volume of oil to meet the Dp_{min} requirements is defined as LC3.

From the parametric model, three different alternatives were generated: C01 (base case), C02 (reduced structural weight), and C03 (higher natural periods of the heave and pitch motions). The alternatives serve to develop the operability criteria based on a parametric discretization. The main characteristics of the three design alternatives are presented in Tables 6 and 7. The main dimensions of the C03 alternative are presented in Fig. 15.

4.4 Stability Analyses. Static stability analysis was carried out for the design alternatives considering intact and damaged conditions. The study was conducted using the software SSTAB® (see Ref. [11]). Stability criteria recommended by the American Bureau of Shipping (ABS) [12] was taken into consideration.

The stability results are illustrated in Table 8 and indicate that the CO2 alternative does not satisfy the damage stability criteria; therefore, this alternative will not be considered in the next design stages.

4.5 First Order Response. The RAOs results for the heave motion of the main body are illustrated in Fig. 16. The RAOs results for the pitch motion of the main body are illustrated in Fig. 17. The RAOs results for the heave motion of the inner body, taking into consideration restoring forces due to the risers, are illustrated in Fig. 18.

It should be pointed out that the results were obtained without taking into consideration the viscous damping since only the potential component was included in the model.

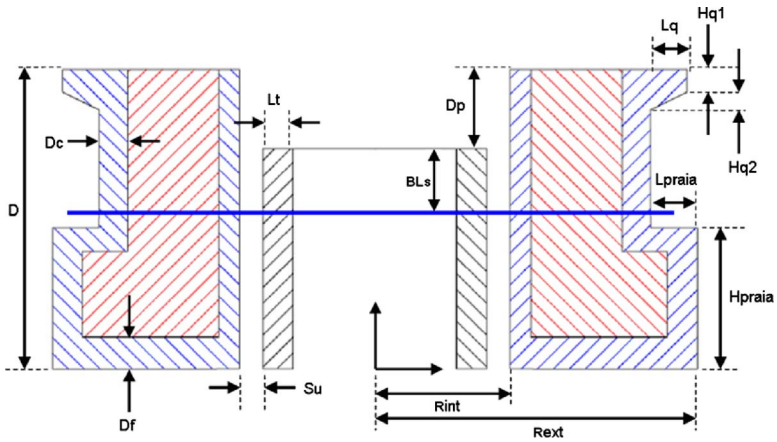

Fig. 12 Design variables

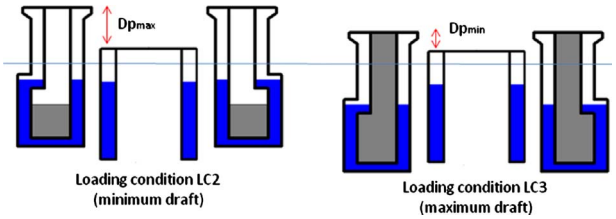

Fig. 13 Loading conditions

The RAO results were used to obtain the significant height for the heave and pitch motions. The significant height was calculated by

$$H_s = 4 \cdot \sqrt{m_0} \tag{2}$$

where

$$m_o = \int_0^\infty S_R(\omega) \cdot d\omega \tag{3}$$

$$S_R(\omega) = S_w(\omega) \cdot \mathrm{RAO}^2(\omega) \tag{4}$$

where m_0 is the zero order moment of the response spectrum, S_R is the response spectrum, and S_w is the wave spectrum obtained by the JONSWAP formulation.

Tables 9 and 10 illustrate the results of the significant heights for the heave motion of the main and inner bodies, respectively. The results were obtained in the frequency domain, considering only the potential damping.

Table 11 illustrates the significant height result for the pitch motion of the main body. The first order heave motions shown by the C03 alternative denote better performance than those in C01 (lower significant heights) in all loading conditions. In the case of the pitch motions, the CO3 alternative also presents better performance; only in the LC2 loading condition does the C01 alternative present lower significant pitch.

As the C03 alternative has shown a better performance, further analysis of the motion response was performed with this configuration. The evaluation of the system motion for the C03 alternative was performed for three different levels of viscous damping for the heave and pitch motions of the main body: $\zeta=2\%$, $\zeta=4\%$, and $\zeta=6\%$; the RAOs results are presented in Figs. 19–21. The viscous damping for the free surface elevation was assumed to be equal to 2%; based on previous experimental results, a viscous damping equal to 6% for the heave motion of the inner body was assumed.

Different damping levels were tested because, as demonstrated by Malta et al. [6], there are terms of coupled damping between the main body and moonpool in the motion equation; thus, it is not easy to estimate the damping coefficients through decay tests of different geometries.

Tables 12 and 13 illustrate the results of the significant height for the heave motion of the main and inner bodies, respectively, considering the different levels of viscous damping. The incorporation of the viscous damping is expected to lead to results closer to the experimental ones.

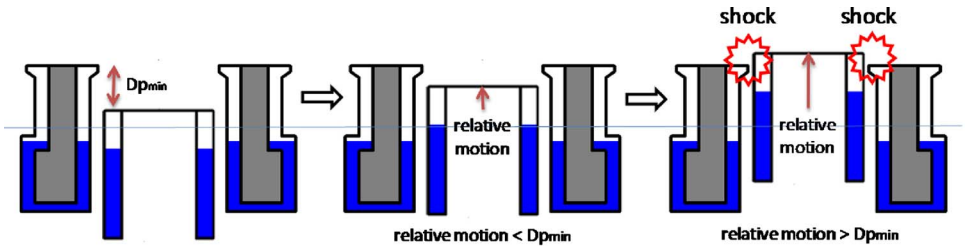

Fig. 14 Example of the relative motion between the bodies

Table 6 Main features of the main body

Case ID	Loading condition	Displacement (m^3)	Draft (m)	GM (m)	Heave period (s)	Pitch period (s)	Oil storage (bbl)	Inertia ($t\ m^2$)	Structural mass (t)
C01	LC1	146,026	26.50	4.96	17.43	37.93	0	$1.94\times10^{+8}$	19,926
	LC2			11.92		24.04	200,775	$1.88\times10^{+8}$	
	LC3	192,445	38.50	11.89	20.01	23.12	244,232	$2.28\times10^{+8}$	
	LC4			9.34		26.18	803,100	$2.30\times10^{+8}$	
C02	LC1	158,023	22.00	1.59	16.77	59.50	0	$1.65\times10^{+8}$	17,640
	LC2			6.43		28.63	204,276	$1.55\times10^{+8}$	
	LC3	212,276	34.00	6.12	19.44	27.48	605,702	$1.83\times10^{+8}$	
	LC4			3.40		36.98	817,103	$1.84\times10^{+8}$	
C03	LC1	150,535	24.00	1.13	17.14	72.61	0	$1.67\times10^{+8}$	17,731
	LC2			7.05		27.99	200,862	$1.55\times10^{+8}$	
	LC3	200,035	36.00	7.17	19.76	26.26	567,121	$1.84\times10^{+8}$	
	LC4			4.30		34.06	803,447	$1.86\times10^{+8}$	

Table 7 Main features of the inner body

Case ID	External diameter (m)	Draft (m)	Displacement (t)	Structural mass (t)	Heave period (s)	Ballast (t)
C01	56.00	30.13	26,650	2,031	9.88	20,000
C02	22.00	26.33	8,902	683	9.29	3,600
C03	34.00	22.92	10,703	1,084	8.92	5,000

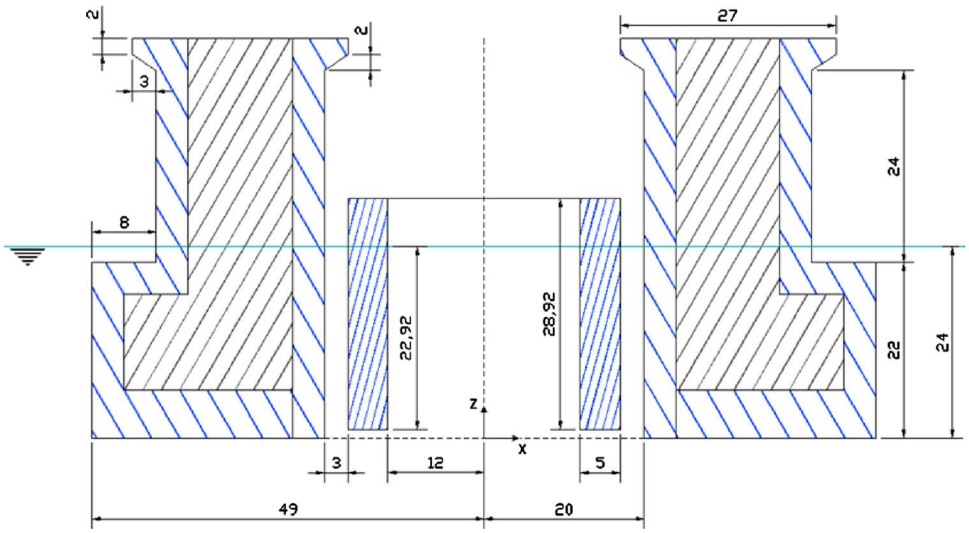

Fig. 15 Main dimensions—C03 alternative

The results for the pitch motion are illustrated in Table 14. There was no difference between the results for the different damping levels because the natural period of pitch is far from the wave spectrum peak. The pitch motion response in the loading condition LC2 is considered great when compared with the response of similar units.

The heave motion of the inner body is relevant since it will determine tensions acting on the risers. Since each point on the deck of the inner body presents a different motion, the deck surface was discretized, and the acceleration of the coupled motion (heave and pitch) of each point was evaluated.

The results for the C03 alternative in the LC2 loading condition, for $\zeta=2\%$, are illustrated in Fig. 22 as a function of gravity acceleration. Since an acceleration equal to 10% of the gravity acceleration is considered acceptable as good machinery performance, and since the results obtained are lower than this, the system performance is satisfactory.

The relative motion between the two bodies is important for the system safety because a great relative motion may cause a collision between two decks or a disconnection of the oil hoses.

The results for relative motions for the C03 alternative are illustrated in Table 15. Only in case of the LC2 loading condition and viscous damping $\zeta=2\%$ does the relative motion exceed 8.0 m, which will cause a shock between the two bodies (see Fig. 14). However, the damping coefficient considered ($\zeta=2\%$) is lower than the damping measured in similar units.

4.6 Low Frequency Surge Motion. The main body second order surge motion is important in order to design the mooring system, because its performance will depend on the system offset.

The offset of the new concept should be small due to the dry completion requirement, which cannot support high tensions. Another problem created by high offsets is the inner body sinkage, which will cause the disconnection of the hoses.

The root mean square (rms) of the second order surge motion, using a damping $\zeta=2\%$, was evaluated according to Ref. [13]. The second order forces were estimated using the WAMIT® code.

Figure 23 illustrates the rms results of the second order surge motion for the CO1 and CO3 alternatives in the survivability conditions of the Campos basin. The results are given for the different stiffnesses of the mooring system.

4.7 Design of the Mooring System. The design takes into consideration the different compositions of the mooring lines. The lines, as previously mentioned, are composed of three parts.

A design procedure proposed by Martins et al. [14] and Andrade et al. [15] was used; the force evaluation and the adopted design criteria are based on the Det Norske Veritas (DNV) rules [16].

The length of the intermediate part of the mooring line, the maximum tension on the lines, the maximum offset, and the anchorage radius were evaluated for a given configuration of the mooring lines, so that the mooring system satisfied the following design requirements: (i) taut-leg system, thus the length of the line part supported on the sea floor equals zero, (ii) maximum offset equals 10% of water depth, and (iii) maximum allowable tension acting on the lines equal to 55.6% of the ultimate strength.

The design environmental condition is defined as the survivability condition, according to the DNV norm. Figure 24 illustrates the forces applied to the platforms for C03 alternative due to the environmental agents (wind, wave, and current).

Different values of the damping coefficient for the surge motion, as shown in Fig. 25, were used to evaluate the performance of the mooring system. A change in the damping coefficient leads

Table 8 Stability results

	Intact condition analyses				Damaged condition analyses			
	ABS rules	Case C01 LC1	Case C02 LC1	Case C03 LC1	ABS rules	Case C01 LC4	Case C02 LC4	Case C03 LC4
Corrected transversal GM (m)	>1.0	5.04	1.44	1.37	-	9.55	6.06	5.74
Area ratio	>1.3	8.11	9.31	7.29	-	7.29	2.22	2.74
Stability range (deg)	-	29.11	35.93	32.55	>7.0	12.14	4.47	7.24
GZ/WHL max	-	15.85	17.66	15.26	>2.0	12.32	4.29	5.54
Status	-	Ok	Ok	Ok	-	Ok	Rejected	Ok

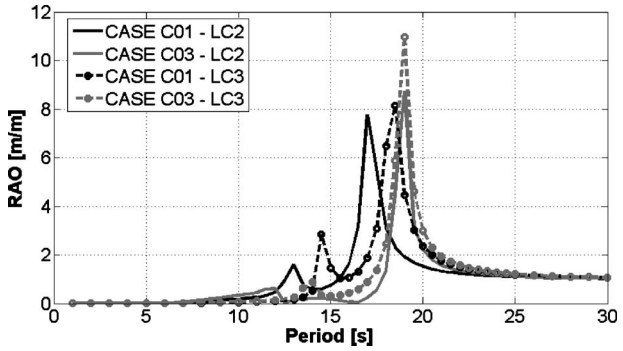

Fig. 16 Heave motion RAOs—main body

to a change in the rms of the second order surge motion.

The line configurations considered to perform the design of the mooring system are illustrated in Fig. 26. A set of feasible solutions provided by the design procedure for the above lines configuration is presented in Fig. 27 for a damping coefficient $\zeta = 2\%$. These solutions are presented in an offset versus anchorage radius graphic.

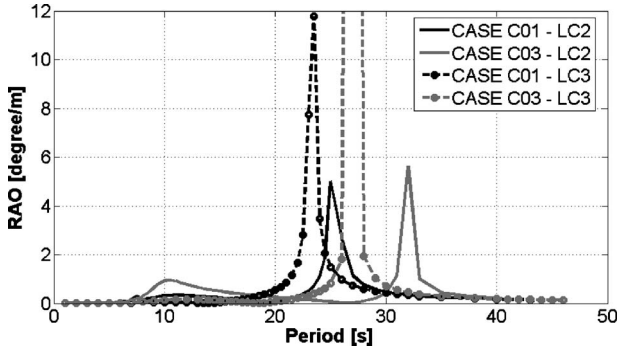

Fig. 17 Pitch motion RAOs—main body

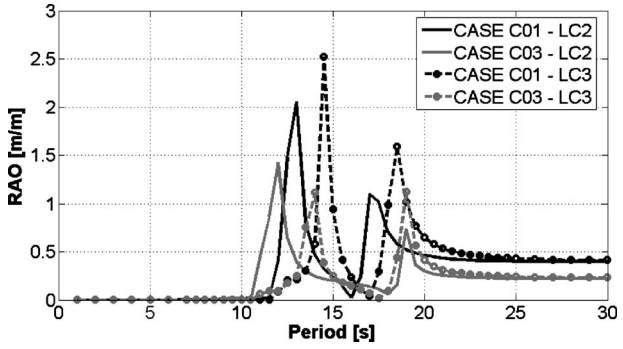

Fig. 18 Heave motion RAOs—inner body with risers, restoring forces

Table 9 Significant height of the heave motion (m)—main body

Case ID	Loading condition	Sea 1	Sea 2	Sea 3
C01	LC2	9.47	12.85	16.49
	LC3	8.77	12.40	15.80
C03	LC2	5.00	7.63	13.71
	LC3	6.66	10.15	13.77

Table 10 Significant height of the heave motion (m)—inner body

Case ID	Loading condition	Sea 1	Sea 2	Sea 3
C01	LC2	4.66	4.87	5.18
	LC3	4.31	5.30	5.73
C03	LC2	2.89	3.05	3.21
	LC3	2.51	2.80	2.96

It can be seen that the offsets in the level of 5% of the water depth are obtained with the adopted configurations, which means that there is a good safety margin with respect to the specified requirement.

5 Hydrodynamic Appendages

The final results showed that the first order motion, mainly the pitch, must be improved. One way to achieve this is by incorporating hydrodynamic appendages (heave plates), as proposed by Thiagarajan and Troesch [17], Thiagarajan et al. [18], and Tao and Cai [19]. This approach results in an increase in the added mass and viscous damping. This is the alternative chosen to be tested herein.

Table 11 Significant height of the pitch motion (deg)—main body

Case ID	Loading condition	Sea 1	Sea 2	Sea 3
C01	LC2	1.65	1.78	1.95
	LC3	0.84	1.89	3.53
C03	LC2	3.99	4.29	4.51
	LC3	0.83	1.05	2.09

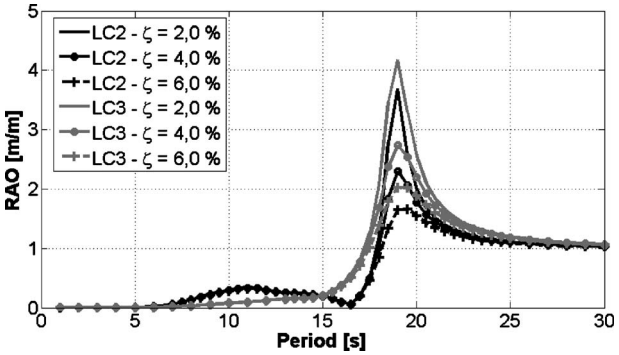

Fig. 19 Heave motion RAOs–including viscous damping–main body

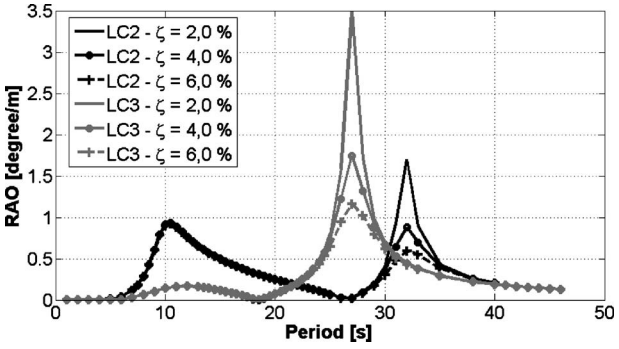

Fig. 20 Pitch motion RAOs including viscous damping—main body

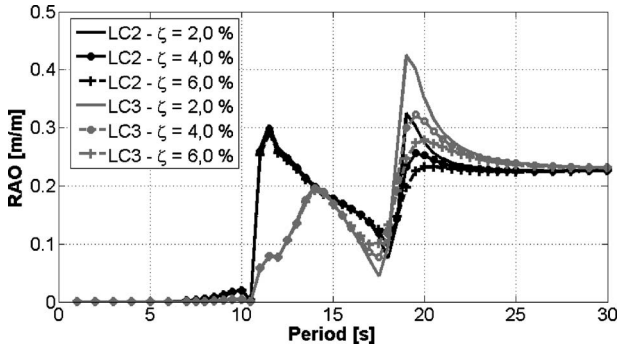

Fig. 21 Heave motion RAOs including viscous damping—inner body

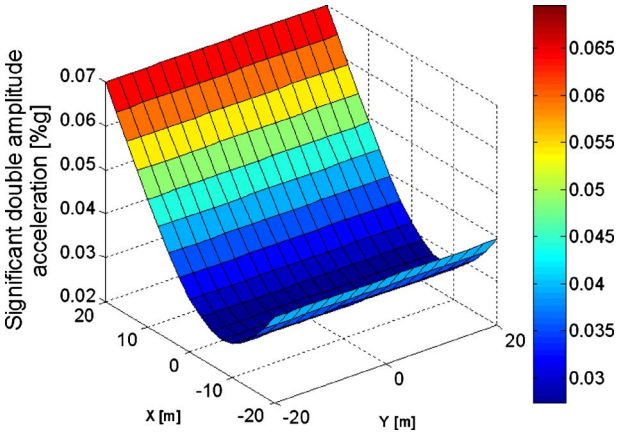

Fig. 22 Significant double amplitude acceleration at deck of the inner body—alternative C03-LC2 loading condition

The use of a device working with the moonpool is proposed to promote an increase in the additional mass and damping to the system. In order to do so, two appendages were utilized: the first is a horizontal disk located at the bottom of the platform, and the second is a circular plate around it, according to Fig. 28.

Prislin et al. [20] examined how the additional mass and drag coefficient of solid square plates, oscillating perpendicularly to their planes in otherwise quiescent fluid, depend on the Keulegan–Carpenter number and on the Reynolds number.

Concerning the monocolumn platform, the main damping contribution comes from drag forces, which shows to be weakly influenced by the Reynolds number. Furthermore, the influence on the added mass due to multiplates was examined, and an optimal spacing between plates was proposed. The appendages presented here are composed of two plates not located on the same plane.

Table 12 Significant height of the heave motion (m) including viscous damping—main body

Viscous damping	Loading condition	Sea 1	Sea 2	Sea 3
ζ=2%	LC2	3.07	4.55	6.12
	LC3	3.70	5.71	7.80
ζ=4%	LC2	2.43	3.48	4.64
	LC3	2.87	4.40	6.01
ζ=6%	LC2	2.10	2.91	3.84
	LC3	2.39	3.63	4.96

Table 13 Significant height of the heave motion (m) including viscous damping—inner body

Viscous damping	Loading condition	Sea 1	Sea 2	Sea 3
ζ=2%	LC2	1.17	1.31	1.44
	LC3	0.81	1.00	1.18
ζ=4%	LC2	1.15	1.21	1.40
	LC3	0.78	0.95	1.10
ζ=6%	LC2	1.13	1.26	1.38
	LC3	0.77	0.93	1.07

Table 14 Significant height of the pitch motion (deg) including viscous damping—main body

Viscous damping	Loading condition	Sea 1	Sea 2	Sea 3
ζ=2%	LC2	3.97	4.27	4.48
	LC3	0.83	0.90	0.97
ζ=4%	LC2	3.97	4.27	4.48
	LC3	0.83	0.90	0.97
ζ=6%	LC2	3.97	4.27	4.48
	LC3	0.83	0.90	0.97

On platforms such as the tension leg platform (TLP), Thiagarajan and Troesch [17] showed the effects of adding an appendage in the form of a disk. Their work has evidenced that the device modified the damping coefficient as well as the additional mass. An example of a full scaled TLP utilized in their work presented a 300% increase in damping.

Four configurations (three with appendages) were tested. A comparison between each configuration was performed, and the results showed a change in the natural period when the appendages were located inside the moonpool. On the other hand, when the appendages were located outside the platform, a significant increase of approximately 4 s in the natural period of the heave motion was noted; details about these tests, including the numerical models, were presented by Matsumoto et al. [21]. Similar experimental tests to evaluate the effects of appendages on a monocolumn were studied by Masetti et al. [22].

The four configurations tested in the tank were as follows:

- platform without appendages (SS)
- platform only with external appendages (CS)

Table 15 Significant height of the relative motion between the bodies (m)

Viscous damping	Loading condition	Sea 1	Sea 2	Sea 3
ζ=2%	LC2	3.45	5.06	6.77
	LC3	4.48	6.80	9.19
ζ=4%	LC2	2.79	3.96	5.19
	LC3	3.41	5.25	7.15
ζ=6%	LC2	2.46	3.35	4.37
	LC3	2.85	4.35	5.93

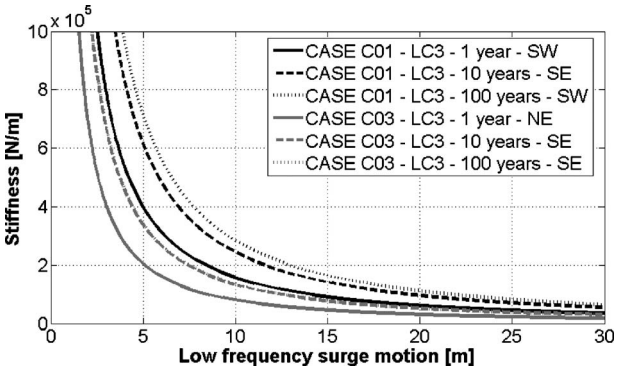

Fig. 23 Low frequency surge motion rms

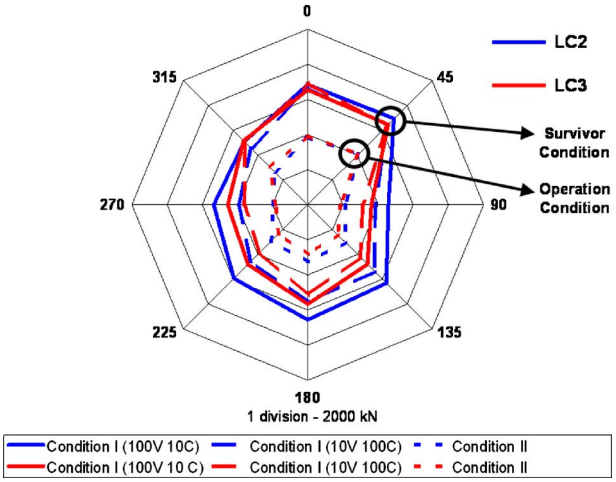

Fig. 24 Static forces on alternative C03

- platform only with internal appendages (SR)
- platform with both external and internal appendages (CR)

The physical model utilized in the experiments was the same as that in the previous tests. The only change is the insertion of the appendages. Figure 29 shows the model with the appendages utilized in the experiments.

For each configuration, a decay test was carried out to get the platform heave and pitch natural periods. The results indicated a great influence of the external appendages and a small influence of the internal ones on the natural period of vertical motions.

The RAO results for the heave and pitch motions, and free surface elevations at the moonpool, were obtained by transient waves. Figure 30 shows the monocolumn RAO results for the heave motion. Clearly, the influence of the external appendage can be verified (CS and CR configurations). The natural heave period and the peak of RAO change considerably, but the influence of the internal appendages (SR and CR) on motion is not as representative as the external one, providing a small attenuation to the resonant region.

Similar to the RAO results for the heave motion, the results for the pitch motion (see Fig. 31) presented a significant modification in the natural period only with external appendages present. The internal appendages induced a small attenuation on the curve peak only in the resonant region.

The motion of the free surface elevation at the moonpool (see Fig. 32) is lower at the SR and CR configurations. In these conditions, the presence of internal appendages attenuates the resonant region of the free surface motion.

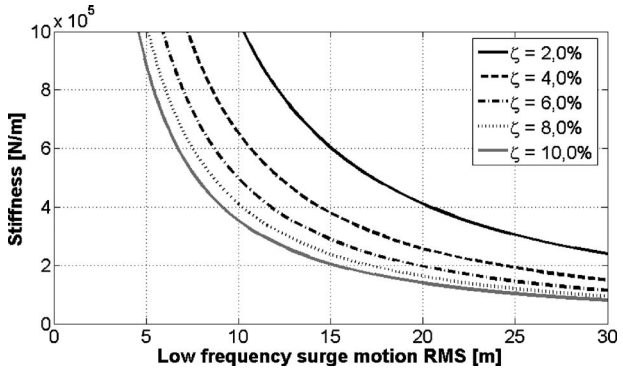

Fig. 25 Different damping coefficients on low frequency surge motion

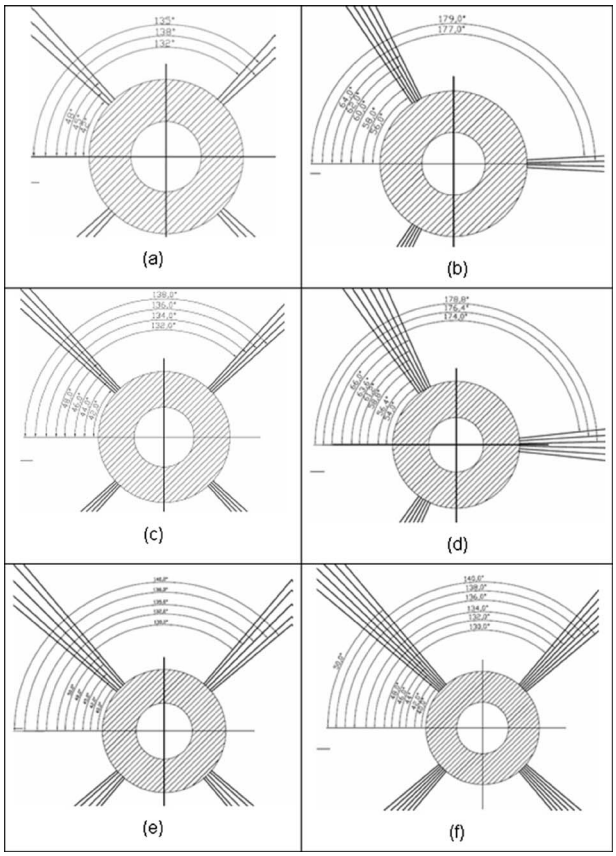

Fig. 26 Mooring line layout: (*a*) 12 lines, (*b*) 14 lines, (*c*) 16 lines, (*d*) 18 lines, (*e*) 20 lines, and (*f*) 24 lines

In conclusion, the use of appendages on a monocolumn platform improves the system dynamic performance, which introduces damping and additional mass on this system.

6 General Conclusions

The new concept of a monocolumn floating production and storage system with dry tree capability can be considered feasible according to the studies presented in this paper.

A detailed study of the body motions and static stability is presented as well, including a parametric model to generate the platform characteristics. A set of model tests were carried out to validate the numerical models, showing a good agreement between the results.

The stability analysis indicated that one of these alternatives (C02) did not meet the static stability requirements specified by the ABS rules.

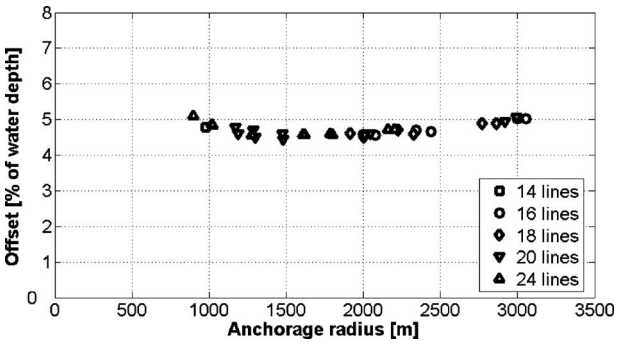

Fig. 27 Feasible solutions of the mooring systems ζ=2%

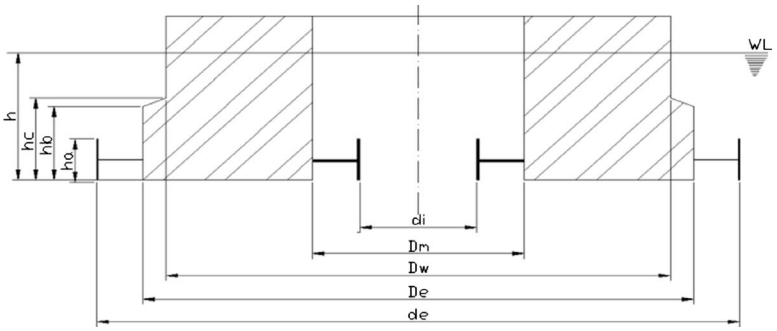

Fig. 28 Main dimension of the hydrodynamic appendage

The study of system dynamic behavior, considering first (heave and pitch) and second order surge motions, and a limited number of parametric studies, indicate that the C03 alternative is superior.

For the best alternative (C03), further analysis of the first order motions was performed, considering the incorporation of realistic viscous damping; the system response was improved. The final results showed that the first order motion, mainly the pitch, must be improved.

Fig. 29 Platform and hydrodynamic appendage models

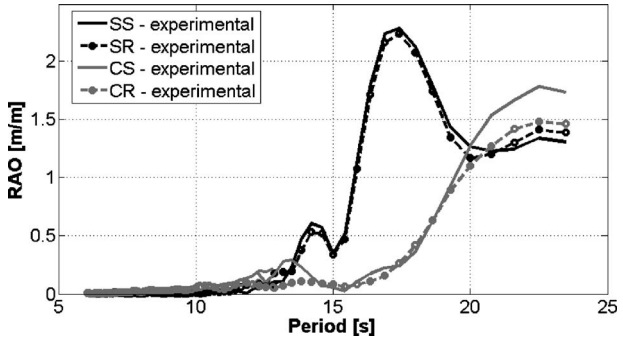

Fig. 30 Heave motion RAOs—hydrodynamic appendage experimental results

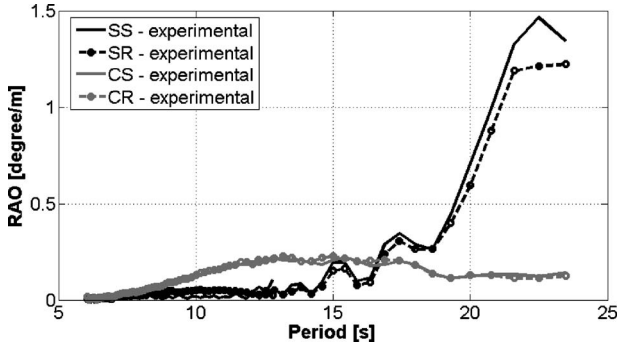

Fig. 31 Pitch motion RAOs—hydrodynamic appendage experimental results

Finally, the design of the mooring system employed for the best alternative (C03) and its results demonstrated the feasibility of the concept, considering 5% of water depth the maximum offset. However, to consolidate this concept, new studies should be carried out. For instance, the second order motion of the platform should be used in the estimation for the first order motion, as it will influence the relative motion between the two bodies.

The entire platform may be optimized, for instance, with the inclusion of hydrodynamic appendages on the main body, which introduces damping and additional mass to this system, providing a substantial change in the natural period of the vertical motion, detuning the platform resonance, and moving it outside the range of wave energy. In addition, the inner body geometry may be changed.

This work should be considered as a starting point for further studies on this new conception.

Acknowledgment

The authors thank the Department of Naval Architecture and Ocean Engineering and the Numerical Offshore Tank (TPN) Laboratory of the University of São Paulo, and PETROBRAS, in particular, Eng. Dr. Isaías Quaresma Masetti. The Department of Naval Architecture provided the trial basin for the experimental tests and the TPN Laboratory provided the computer facilities and software. PETROBRAS provided the platform models.

Nomenclature

γ = peakedness parameter
ω = wave frequency (rad/s)
ζ = damping coefficient
BL_s = inner body freeboard (m)
C02 = case ID C02
C03 = case ID C03
D = depth (m)
Dc = double side (m)

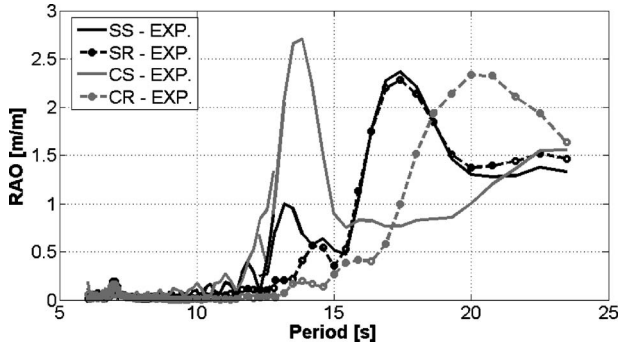

Fig. 32 Free surface elevation at moonpool RAOs—hydrodynamic appendage experimental results

De = external diameter below water line (m)
Df = double bottom (m)
Dm = moonpool diameter (m)
Dp = difference between decks (m)
Dp_{max} = maximum difference between decks (m)
Dp_{min} = minimum difference between decks (m)
Dw = water line external diameter (m)
de = external diameter of the external appendage (m)
di = internal diameter of the external appendage (m)
GM = metacentric height (m)
GZ = righting moment curve
h = draft (m)
ha = external appendage height (m)
Hpraia = main body beach height (m)
H_s = significant height (m)
LC2 = loading condition LC2 (minimum draft)
LC3 = loading condition LC3 (maximum draft)
Lpraia = main body beach width (m)
Lt = inner body ballast tank width (m)
m_0 = zero order moment of spectrum (m^2)
$RAO_{moonpool}$ = moonpool elevation motion RAO (m/m)
RAO_{inner} = inner body heave motion RAO with main body (m/m)
RAO^*_{inner} = inner body heave motion RAO itself (m/m)
Rext = main body external radius (m)
Rint = main body internal radius (m)
Su = space between bodies (m)
S_R = response spectrum (m^2 s)
S_w = rea or wave spectrum (m^2 s)
T_p = peak period (s)
WHL = wind heeling moment curve

References

[1] Poldervaart, L., and Pollack, J., 2002, "A Dry Tree FPDSO Unit for Brazilian Waters," Proceedings of the Offshore Technology Conference—OTC 2002, Houston, TX.
[2] Reyes, M. C. T., Alho, A. T. P., Kaleff, P., and Masetti, I. Q., 2009, "Dry Wellhead Completion for Mono-Column FPSO Units Operating in Ultradeep Waters," Proceedings of the 28th International Conference on Ocean, Offshore and Arctic Engineering, Honolulu, HI, Paper No. OMAE 2009-79586.
[3] Masetti, I. Q., Costa, A. P., Goulart, R. O., Nishimoto, K., Cueva, M., and Cueva, D., 2006, "General View About the Design of Monocolumn Floaters," Proceedings of the Rio Oil and Gas 2006, Paper No. IBP1749/06.
[4] Sphaier, S. H., Torres, F. G. S., Masetti, I. Q., Costa, A. P., and Levi, C., 2007, "Monocolumn Behavior in Waves: Experimental Analysis," Ocean Eng., **34**, pp. 1724–1733.
[5] IMO, 1997, *MARPOL 73/78: Articles, Protocols, Annexes, Unified Interpretations of the International Convention for the Prevention of Pollution From Ships, 1973, as Modified by the Protocol of 1978 Relating Thereto*, International Maritime Organization, London.
[6] Malta, E. B., Cueva, M., and Nishimoto, K., Gonçalves, R. T., and Masetti, I., 2006, "Numerical Moonpool Modeling," Proceedings of the 25th International Conference on Offshore Mechanics and Arctic Engineering, Hamburg, Germany, Paper No. OMAE2006-92456.
[7] Torres, F., 2007, "Study of Numerical Modeling of Moonpool as Minimization Device of Monocolumn Hull" (in Portuguese), MS thesis, University of São Paulo, São Paulo, Brazil.
[8] Torres, F., Cueva, M., Malta, E. B., Nishimoto, K., and Ferreira, M. D., 2004, "Study of Numerical Modeling of Moonpool as Minimization Device of Monocolumn Hull," Proceedings of the 24th International Conference Offshore Mechanics and Arctic Engineering, Vancouver, Canada, Paper No. OMAE 2004-51540.
[9] Wamit, Inc., 2003, WAMIT® User Manual, Versions 6.2, 6.2PC, 6.2S, 6.2S-PC.
[10] Malta, E. B., Santos, B. M. R., Rampazzo, F. P., Campos, F. C. R., Prado, M. A., and Koga, R. A., 2004, "Conceptual Design of Itapoa Platform," Proceedings of the ISODC 2004.
[11] Tecgraf, Inc., 2002, *SSTAB® User Manual-Version 2.43—Floating Systems Stability and Ballast Control (in Portuguese)*, Pontifícia Universidade Católica do Rio de Janeiro, Rio de Janeiro.
[12] ABS, 2006, *ABS Guide for Building and Classing-Mobile Offshore Drilling Units*, American Bureau of Shipping, Houston, TX, USA.
[13] Aranha, J. A. P., and Fernandes, A. C., 1994, "On the Second Order Slow Drift Force Spectrum of a Floating Body," Appl. Ocean Res., **17**(5), pp. 311–313.
[14] Martins, M. R., Brinati, H. L., and Andrade, B. L. R., 1997, "A Comparative Study of the Conventional and Taut-Leg Mooring System," Proceedings of the 1997 International Conference Offshore Mechanics and Arctic Engineering—OMAE 1997, Yokohama, Japan.
[15] Andrade, B. L. R., Martins, M. R., and Brinati, H. L., 1997, "A Synthesis Procedure of Mooring System to Reduce Costs and Simplify the Underwater Layout," Proceedings of the Seventh International Offshore and Polar Engineering Conference—ISOPE 1997, Honolulu, HI.
[16] DNV, 1989, *POSMOR-Position Mooring*, Det Norske Veritas, Hovik, Norway.
[17] Thiagarajan, K. P., and Troesch, A. W., 1998, "Effects of Appendages and Small Currents on the Hydrodynamic Heave Damping of TLP Columns," ASME J. Offshore Mech. Arct. Eng., **120**, pp. 37–42.
[18] Thiagarajan, K. P., Datta, I., Ran, A. Z., Tao, L., and Halkyard, J. E., 2002, "Influence of heave Plate Geometry on the Heave Response of Classic Spar," Proceedings of the 22nd International Conference Offshore Mechanics and Arctic Engineering, Oslo, Norway, Paper No. OMAE 2002-28350.
[19] Tao, L., and Cai, S., 2004, "heave Motion Suppression of a Spar With a Heave Plate," Ocean Eng., **31**(5–6), pp. 669–692.
[20] Prislin, I., Blevins, R., and Halkyard, J., 1998, "Viscous Damping and Added Mass of Solid Square Plates," Proceedings of the 1998 International Conference Offshore Mechanics and Arctic Engineering—OMAE 1998, Lisbon, Portugal.
[21] Matsumoto, F. T., Gonçalves, R. T., Malta, E. B., Medeiros, H. F., Nishimoto, K., and Masetti, I. Q., 2008, "The Influence at Vertical First Order Motions Using Appendages in a Monocolumn Platform," Proceedings of the 27th International Conference on Offshore Mechanics and Arctic Engineering, Estoril, Portugal, Paper No. OMAE 2008-57410.
[22] Masetti, I. Q., Costa, A. P., Matter, G. B., Barreira, R. A., and Sphaier, S. H., 2007, "Effect of Skirts on the Behavior of a Mono-Column Structure in Waves," Proceedings of the 26th International Conference on Offshore Mechanics and Arctic Engineering, San Diego, CA, Paper No. OMAE2007-29024.